Journal of Chromatography A 1689 (2023) 463756

Contents lists available at ScienceDirect

Journal of Chromatography A

journal homepage: www.elsevier.com/locate/chroma

Performance of global retention models in the optimisation of the chromatographic separation (I): Simple multi-analyte samples

P. Peiró-Vila[a], M.D. Villamonte[b], I. Luján-Roca[a], J.R. Torres-Lapasió[a,*], M.C. García-Alvarez-Coque[a]

[a] Department of Analytical Chemistry, Faculty of Chemistry, Universitat de València, C/ Dr. Moliner 50, Burjassot 46100, Spain
[b] Instituto de Investigaciones Biológicas, CONICET, Universidad Mar de Plata, Argentina

ARTICLE INFO

Article history:
Received 26 October 2022
Revised 23 December 2022
Accepted 23 December 2022
Available online 29 December 2022

Keywords:
Global retention models
Multi-linear gradient elution
Optimisation of resolution
Multi-analyte samples
Modelling of unknowns

ABSTRACT

Conventional retention models lead to accurate descriptions of the elution behaviour from the fitting of data for single solutes or from a set of solutes, one by one. However, the simultaneous fitting of several solutes through a regression process that separates the contributions of column and solvent from those of each solute is also possible. The result is a global retention model constituted by a set of equations with some common parameters (those associated with column and solvent), whereas others, specific to each solute, differ for each equation. This work explores the possibilities, advantages, and limitations of global models when they are applied to the optimisation of chromatographic resolution. A set constituted by 13 drugs (diuretics and β-blockers) and a training experimental design of seven multi-linear gradients are considered. Since standards for all compounds were available, the optimisation based on global models could be compared with the conventional optimisation, which is based on individual models. In their current state, global models do not predict changes in elution order, but they do allow for incorporating additional solutes (e.g., new analytes or matrix peaks) with only one new experiment. This possibility is explored by extending the model for the 13 analytes to include 26 peaks associated with a contamination in the injector. The combination of individual and global models allows an optimisation where the effects of matrix peaks on the separation of analytes can be integrated.

1. Introduction

In liquid chromatography, finding the best mobile-phase composition that balances satisfactory peak resolution, and convenient analysis time, may be a difficult task. In many samples, even when they are relatively simple, protocols based on trial and error can be too laborious and often unsuccessful. Fortunately, method development can be highly improved using computer strategies, where the resolution or retention behaviour of the sample components are modelled to further predicting the best separation conditions [1–4]. In order to achieve better performance, efforts have been invested in several related topics: (i) quality of the source data (number, distribution and elution mode of the experiments within the experimental design) [5–8]; (ii) accuracy of the description of retention using empirical or mechanistic models [9–13]; (iii) development of chromatographic objective functions (COFs) expressing the quality aims that the chromatographer pursuits [14–19], and (iv) mathematical strategies to simulate chromatograms and find the most suitable conditions [3,4,20,21]. Modelling of retention is usually the most critical and time-consuming step, being thus the reliability of the models of paramount importance.

The factor most frequently optimised is the organic modifier content in the mobile phase or its changes during the elution process. This preference is due to its large impact on both elution strength and selectivity, and the fact that it can be easily and accurately changed over wide ranges. This justifies the importance of having reliable models to describe the retention that involve only this factor. Snyder et al. [22], Schoenmakers et al. [23], Neue and Kuss [24], Bosch et al. [25], and Jandera et al. [26] have proposed equations that are used to describe the retention in reversed-phase liquid chromatography (RPLC). Classically, each of these equations is individually fitted using the retention data from several elution conditions associated with the same solute, to describe its behaviour in the sample. In this way, individual fits of retention data lead to specific values of the model parameters for each solute. Another perspective, explored in Refs. [27–29], consists of developing

* Corresponding author.
E-mail address: jrtorres@uv.es (J.R. Torres-Lapasió).

https://doi.org/10.1016/j.chroma.2022.463756

a "global model", that is, an equation (or a set of equations sharing parameters) that describes the behaviour of several compounds simultaneously by establishing the general behaviour of the chromatographic system. With global models, the retention behaviour of known or unknown solutes can be predicted, with some limitations. Individual models offer more accurate descriptions, because these can describe the specifics of the retention behaviour of the individual solutes, but cannot be applied to other solutes. Other type of global models used in chromatography are the so-called hierarchical or multi-level models, where a regression based on a Bayesian approach is applied to a training set of solutes with known QSRR parameters [30,31].

We have recently proposed a methodology for the prediction of chromatograms for highly complex samples containing unknown constituents, such as medicinal plant extracts [27–29]. In the published reports, we developed a strategy for building a global model, which separates the contributions of column and solvent from those of each solute in the sample. The strategy is based on the application of a fitting algorithm that associates some parameters to the separation environment, whereas other parameter(s) are associated to each solute according to their particular nature. The process implies the treatment of the retention data of all solutes and separation conditions in the experimental design, simultaneously. The global model can be easily extended to include additional compounds with minimal experimental effort.

This work explores and discusses the features, advantages and limitations of an optimisation based on the approach described in Ref. [27] to fit global models compared to a conventional optimisation, which is based on individual models. For this purpose, the retention data for a relatively simple sample, for which standards were available, was fitted with both individual and global models. The chromatograms included also some additional peaks of unknown impurities, not associated to the sample but to the injector. The experimental design consists of six multi-linear gradients, where one of the nodes has variable position, following a rhomboidal geometry. This allows accommodating the retention of compounds with very different hydrophobicity within similar time scales. The fitted global model, initially developed for the 13 analytes and degradation products, was further extended to include 26 additional peaks coming from the injector.

The study was carried out using a synthetic sample consisting of nine diuretics and two β-blockers, for which there were standards available in our laboratory, together with the impurities of two of the assayed diuretics (two thiazides). Using global retention and peak profile models, predictions of chromatograms were made, including: (i) exclusively the 13 target compounds, or (ii) all constituents in the chromatogram (analytes and injector impurities), accounting in total 39 peaks. The two optimisations were carried out by exploring the expected separation performance of a random population of gradients, which was evolved using Genetic Algorithms (GA) [32,33]. Finally, those conditions among the whole set of explored gradients, for which the best results could be expected in terms of resolution and analysis time, were selected. It is demonstrated that the complete optimisation methodology, which includes a stepwise development of the experimental design, the fitting of global and individual models, and the optimisation of the separation, may offer satisfactory results.

2. Theory

2.1. Modelling of the chromatographic behaviour

We will use the term "restricted global model" to refer to those retention models that simultaneously describe the behaviour of a reduced set of solutes in the sample (the training set). For these solutes either there are standards available, or at least, their peaks can be unambiguously established by peak tracking procedures, among chromatograms corresponding to different experimental conditions, even when their identity is unknown. In practice, these unknown compounds are used as if they were standards, and will be called "reference compounds". The restricted global model is later extended to include all the constituents of the chromatogram (the reference compounds and the remaining components), giving rise to the "extended global model".

This work generalises an equation proposed by Neue-Kuss to describe the retention in RPLC [24], in order to develop a global model. In isocratic elution, the retention time ($t_{R,i}$) of compound i for a modifier concentration φ is calculated as follows:

$$t_{R,i} = t_0 + (t_0 - t_{ext})10^{(\log k_{0,i})}(1 + c\varphi)^2 e^{\frac{-b\varphi}{1+c\varphi}} \quad (1)$$

In Eq. (1), t_0 is the dead time (elution time of an unretained compound) that depends on the organic solvent content, and t_{ext} is the extra-column time associated with the transit of solutes through the tubing from the injector to the detector, excluding the column; ($\log k_{0,i}$), b and c are thus the model parameters. Expressions like Eq. (1), fitted solute by solute, will be called here "individual models" (one per solute, b_i and c_i being thus specific for each solute i), while the restricted global model can be expressed as a set of equations (one equation per solute) with common parameters. In the case of the Neue-Kuss global model, b and c are assumed to be identical for all solutes, while ($\log k_0$) takes different values for each solute.

When the separation is carried out in gradient elution, a straightforward algebraic solution is only possible with simple gradients and for very few models. In situations where there are no direct expressions for t_g, the so-called "fundamental equation for gradient elution" should be solved numerically. The gradient retention time can be obtained from the dependence of the retention factor on the gradient program, $k(\varphi(t))$, by working out t_g from the upper limit of the integral, using zero search methods [34]:

$$t_0 - t_{ext} = \int_0^{t_d} \frac{dt}{k(\varphi_0)} + \int_{t_d}^{t_g - t_0} \frac{dt}{k(\varphi(t))} = \frac{t_d}{k_0} + I(t_g - t_0) - I(t_d) \quad (2)$$

In Eq. (2), t_d is the dwell time, which accounts for the delay in the gradient front to reach the column inlet. In multi-linear gradients, the retention is described including a series of integral terms corresponding to the different consecutive linear segments in the gradient (as many as those the solute crosses until its elution):

$$t_0 - t_{ext} = \int_0^{t_d} \frac{dt}{k(\varphi_0)} + \int_{t_d}^{t_1} \frac{dt}{k(\varphi_1(t))} + \ldots + \int_{t_{n-1}}^{t_g - t_0} \frac{dt}{k(\varphi_n(t))} = \\ = \frac{t_d}{k_0} + \sum_{i=1}^{n-1} (I(t_{i+1}) - I(t_i)) + I\left(t_g - t_0\right) - I(t_{n-1}) \quad (3)$$

As pointed out, numerical methods are often required to obtain the retention time in gradient elution, since algebraic solutions are often impractical or do not exist. In the research presented below, the gradients were always multi-linear, so numerical calculation was the only alternative.

Although the global model is actually a set of equations with common terms, these can be represented in a compact way by a vector $\boldsymbol{p}$, which contains the set of parameters [b, c, $\log k_{0,1}$, $\log k_{0,2}$, …, $\log k_{0,ns}$]. The algorithm applied to carry out the alternate fitting is described in Ref. [27] and summarised in the Supplementary material.

The global model obtained from the training set of solutes with known identity (i.e., the restricted global retention model) allows predictions of the retention times exclusively for these solutes, under any gradient conditions. However, the chromatograms may contain other external solutes besides the analytes. The procedure to extend the restricted global model to include these exter-

nal solutes, giving rise to an "extended global model", is also described in the Supplementary material. The extension of the model requires the selection of the chromatogram in the experimental design showing the maximal number of constituents, which has been called "base chromatogram", usually obtained with the slowest gradient in the design.

In this work, the position, bandwidth, area, and other properties of all visible peaks in the base chromatogram were automatically detected, and measured, using a Matlab function developed in our laboratory, suitable for analysing highly complex chromatograms in an unsupervised fashion [35]. It includes a previous step for automatic baseline subtraction, by applying the BEADS algorithm [36].

Note that the effect of the modifier on retention is determined considering simultaneously several representative solutes, using the retention data of a set of gradients with very different profile. The effect of the hydrophobicity of each solute (ideally independent of the mobile phase), is obtained with the gradient of the experimental design that offers the largest number of peaks. Thus, the prediction of retention for any other arbitrary gradient is possible from parameters *b, c* and log $k_{0,i}$. To do this, the vector that includes the parameters of the global model [*b, c*, log $k_{0,1}$, log $k_{0,2}$, …] is reorganised into a smaller subset of vectors [*b*, *c*, log $k_{0,i}$], each one corresponding to the individual retention model of a given solute.

2.2. Optimisation of the resolution for complex chromatograms

The keystone of model-based optimisation methods in liquid chromatography is the prediction of the quality of the separation by means of the so-called chromatographic objective functions (COFs). These mathematical expressions quantify the separation usually from simulated signals, by assessing performance qualifiers that are targeted for improvement. As a consequence, two COFs may score the same set of chromatograms in a different way, leading to different best separations. Indeed, some COFs correlate better than others with the assessment of quality of an expert analyst. In this work, peak purity, which is defined as the percentage of peak area free of interference, was selected as the COF to measure the chromatographic resolution [14–19]. Peak purity for solute *i* can be easily calculated by simulation, relating the area of peak *i* free of interference from the other components in the chromatogram, with regard to the total area of peak *i* (see Fig. S1 in the Supplementary Material).

The simulation of chromatographic peaks (see Supplementary Material), including the asymmetry, was based on retention models (individual or global) and global half-width models estimated from the equivalent isocratic times at the compositions where each solute leaves the column under the gradient [37–40]. Normalised areas, identical for all peaks, can be used in the prediction of chromatograms when general separation conditions are required. In other situations, as happens in samples where analytes have peaks with dissimilar magnitude, more realistic separations are obtained when experimental areas are used to scale the peaks. This allows better estimations of the separation performance when peaks very different in magnitude are present in the chromatogram.

After evaluating the peak purity of each constituent from simulations, a vector of values with as many elements (p_i) as constituents, $\boldsymbol{r} = [p_1, p_2, \ldots p_{ns}]$ is available for each gradient under evaluation. The p_i elements can be weighted to reflect the importance of each constituent in the separation. Finally, the original (or weighted) p_i measurements are combined into a single value: the overall purity of the whole chromatogram, which is monitored as a guide to drive the optimisation algorithm towards the gradient program offering the best separation.

In this work, with a limited number of constituents, the product of purities will be considered as the global COF. However, in situations with a high number of constituents (some of which may be unresolved under any assayed condition), the sum of purities is more appropriate. Note that when $p_i = 0$ for at least one of the peaks, under all assayed conditions, the product of purities would be so low (zero or close to zero) that distinguishing the separation performance under different peak patterns would not be possible, since the COF will only express the lack of resolution of the fully overlapped peaks.

3. Experimental

3.1. Probe compounds

Nine diuretics and two β-blockers were considered. The diuretics were: ethacrynic acid, benzothiazide, bumetanide, furosemide, probenecid, and trichloromethiazide (Sigma, St. Louis MO), bendroflumethiazide (Davur, Madrid), chlorthalidone (Giba Geigy, Barcelona), and piretanide (Cusi, Barcelona). The β-blockers were: propranolol (Sigma) and oxprenolol (Giba Geigy). Table 1 lists the chemical structures and other relevant properties of the probe compounds. This solute set constitutes an artificial problem with available standards, and therefore, the identity of the peaks at different elution conditions could be easily established. With this mixture, an optimisation of the separation was carried out based on individual and restricted global models, to explore the relative performance.

Two of the diuretics (bendroflumethiazide and trichloromethiazide) were appreciably degraded by the exposition to light and acidity, giving rise to two secondary peaks. These peaks were also included in the training set and modelled together with the pure compounds. Each drug was dissolved in 5 mL of HPLC-grade acetonitrile (Scharlau, Barcelona, Spain), with the assistance of an ultrasonic bath. The initial solutions of the probe compounds were diluted with water to reach 100 µg/mL in the stock solution, except for probenecid, bendroflumethiazide, benzothiazide, and bumetanide, whose concentration was increased to 250 µg/mL, to compensate their lower response.

The stock solutions were stored in the dark at 4 °C. To minimise the effect of the differences in peak area between compounds, solutions of intermediate concentration were prepared by adding the required volume of each standard to a volumetric flask and filling up to the mark. These solutions were filtered into the autosampler vials, using 0.45 mm pore size filters.

3.2. Apparatus and column

The chromatograms were acquired with an Agilent Technologies (Waldbronn, Germany) instrument, which included the following modules: quaternary pump (1260 Series), autosampler (1200 Series) with 2 mL vials, thermostatted column compartment (1200 Series), and diode array UV-visible absorption detector (1260 Series). The system was controlled via an Agilent OpenLAB CDS LC ChemStation (version C.01.08).

A Zorbax Eclipse XDB-C18 column (150 mm × 4.6 mm and 5 mm particle size) was used, protected with a Spherisorb C18 precolumn (30 mm × 4.6 mm, also with 5 mm particles). All injections were performed at controlled temperature (25°C). The injection volume was 10 µL and the mobile phase flow-rate was maintained at 1.0 mL/min.

3.3. Experimental conditions

The analysis of the mixture of diuretics and β-blockers was carried out using acetonitrile gradients, generated with the quaternary pump. HPLC-grade acetonitrile (Scharlau) and nanopure wa-

Table 1
Diuretics ([a]) and β-blockers ([b]) in the studied sample used as training set to develop and compare chromatographic optimisations based on individual and restricted global model. Compounds are listed in order of increasing retention according to the scouting gradient (the identification codes ([c]) are used in the figure tags). Octanol-water partition coefficients (log $P_{o/w}$) and pK_a values were taken from Refs. [41,42].

Compound	Code [c]	Structure	log $P_{o/w}$	log $P_{o/w}$	pK_a
Bendroflumethiazide [a]	BENF	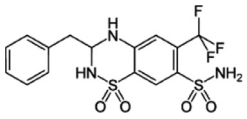	1.95	1.95	9.0
Chlorthalidone [a]	CHLO	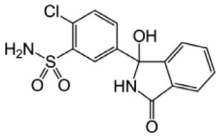	0.24	1.22	9.3
Oxprenolol [b]	OXP	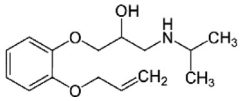	1.83	2.07	9.5
Propranolol [b]	PROP	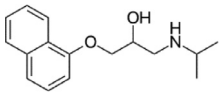	2.60	2.97	9.5
Trichloromethiazide [a]	TRI	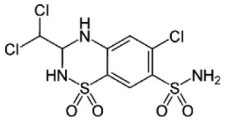	1.0	1.11	7.3, 8.6, 10.6
Furosemide [a]	FUR	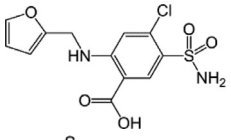	1.81	1.77	3.8, 7.5
Benzothiazide [a]	BENZ	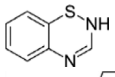	1.73	1.56	6.0
Piretanide [a]	PIR	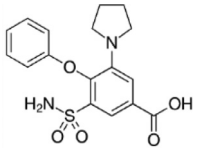	2.20	2.66	4.1
Bumetanide [a]	BUM	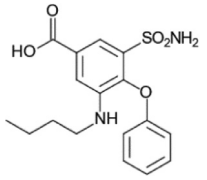	2.09	3.45	3.6, 7.7
Probenecid [a]	PROB	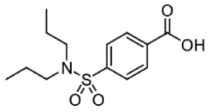	1.40	2.93	3.4
Ethacrynic [a]	ETA	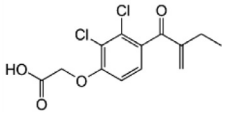	2.28	3.44	3.5

ter (Adrona B30 Trace purification system, Burladingen, Germany) were used in the preparation of the eluents. Gradients were generated by mixing pure acetonitrile with citric acid/dihydrogen citrate buffer containing 20% (v/v) acetonitrile. The buffer was prepared by mixing the appropriate amount of an aqueous solution of citric acid (Panreac, Barcelona) with acetonitrile, and adding NaOH (Scharlab, Barcelona) until reaching pH 3.0, using a previously standardised electrode in aqueous medium (pH_s^W scale). The buffer concentration level was 0.035 M. Gradients included additional column clean-up and stabilisation steps, needed to recondition the separation system before making the next injection. All these solutions, as well as the compounds to be analysed, were filtered through 0.45 µm Nylon membranes before being injected in the chromatographic system. The mobile phases were vacuum filtered and subsequently degassed using an ultrasonic bath from Elmasonic (Singen, Germany). Detection was initially carried out at 254 nm, but it was changed to 274 nm along the study (see Fig. 1), to improve the sensitivity.

The dead time was determined for different mobile phases by injecting KBr (Acros Organics, Geel, Belgium). The dwell time was measured using an acetone gradient (Scharlau), being t_d = 1.167 min. The extra-column time was 0.052 min.

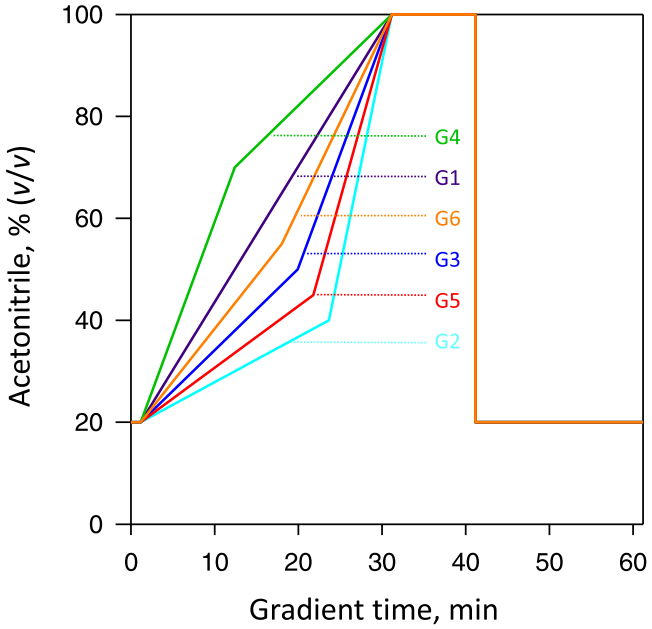

Fig. 1. Experimental design used to fit the retention and peak profile models for the mixture of diuretics and β-blockers (see Table 1). Labels "G1" to "G6" correspond to the acquisition order of the experiments. Once each gradient was completed, 100% acetonitrile was kept during 10 additional minutes to elute incidental highly hydrophobic compounds (contaminants coming from the injector), which could remain in the column. Finally, the acetonitrile level was returned to 20%, which was held for 20 min for column re-equilibration. G1 and G2 experiments were measured at 254 nm, and G3 to G6 at 274 nm to increase the sensitivity.

For the measurement of the peak properties (retention time, half-widths, etc.), and for all calculations involved in the prediction of chromatograms, appropriate home-built functions were developed in the laboratory in Matlab 2020a (The MathWorks Inc., Natick, MA, EE.UU.). No external toolboxes were used.

4. Results and discussion

4.1. Experimental design and analysed sample

In this research, a special type of experimental design has been used, consisting of a set of six multi-linear gradients. Each gradient was differentiated by two consecutive linear segments with different slopes, connected by a node, whose position changes between experiments following a diagonal line, as shown in Fig. 1. This type of design has two interesting advantages [7]:

(i) It allows the elution of components with very different hydrophobicity, without giving rise to excessively long retention times for the most hydrophobic compounds, or resulting in retention times that are too short for the most hydrophilic, even for samples including compounds of extreme hydrophobicity.
(ii) It facilitates peak tracking under different gradients, even in cases where the peak areas cannot be controlled.

However, the coincidence of compositions at very short or long times for different gradients is a drawback, since predictions are limited to the solvent domain covered by the extreme gradients, although this does not imply serious consequences. For unknown samples, the design is sequentially constructed by adding gradients in a stepwise fashion, starting from the information provided by a scouting linear gradient, which covers a wide solvent range. The other gradients are bilinear, obtained by replacing the scouting ramp by two consecutive segments of different slope, and are proposed in a sequence built by gradually altering the slopes attending to the observed results (see Ref. [28]). For known samples, this process can be simplified and the sequence allows more drastic changes (see Fig. 1).

It is worth mentioning that the chromatograph had been inactive for a long period of time. When the instrument was prepared for the first injection, a number of unexpected peaks were found, together with the standards and degradation products. These anomalous peaks were highly reproducible in position and intensity, regardless of the injected composition (sample, blank, or buffer solution). The anomalous peaks were even visible when pure acetonitrile was injected. Fig. 2 shows three overlaid chromatograms, all of them eluted with the scouting gradient (G1 in Fig. 1). Each chromatogram included a group of three or four standards, which are indicated in the figure with the same colour. Note the presence of additional identical peaks in the three injections, which are highly reproducible in position and intensity, being some of them as intense as the peaks of the analytes, whereas others produce broad bands.

The persistence of such peaks suggested that the origin of the contamination was the injector. The manufacturer recommended the replacement of the injector needle and seat, but meanwhile we decided to take advantage of the presence of the reproducible peaks in the contamination background, to enrich the research, checking whether a global model could also explain the elution of unknown compounds associated with the injector contamination (see Section 4.4).

4.2. Modelling the retention using individual and global models

The retention data, obtained with the six training gradients in the experimental design, were fitted solute per solute to Eq. (3) using $k(\varphi)$ in Eq. (1) as retention model and the information of the experimental gradient programs $\varphi(t)$ shown in Fig. 1, in order to obtain the individual models. Meanwhile, the global model for the set of 11 standards and the two peaks associated with the degradation of thiazides was built using the alternate regression strategy described in Ref. [27] and the Supplementary material.

Fig. 3 shows the prediction performance of both types of models (individual and global), considering all solutes and gradients, simultaneously. It can be seen that both types of model provide an excellent predictive capability, although as expected, the predictions with the global model are slightly less precise than those based on a specific modelling for each solute. Table 2, which includes the solutes sorted according to their elution with the scouting gradient, allows a more detailed inspection of the prediction performance. The mean deviation (difference between predicted and experimental retention times in absolute values, considering the six experiments in the design) is usually below 0.1 min with the global models, and somewhat better with the individual models. Relative deviations (with regard to the mean retention) tend to improve with solute hydrophobicity when global models are used, a trend not observed with the individual models. Note the differences between the b and c parameters when they are fitted solute by solute with regard to their values in the global model. This variability, which is a consequence of the scale in k values in the Neue-Kuss equation (in other models the relationship with the organic solvent is logarithmic), makes finding representative values by averaging difficult. In equations with logarithmically transformed retention factors, such as happens with the Snyder's [22] or Schoenmakers' [23], the similarity between slopes (or other parameters) for the individual fits is more evident.

The compounds that present an uncertainty poorer than expected with the global model are those with abnormal changes in selectivity. In the studied sample, these compounds are bendroflumethiazide, propranolol, trichloromethiazide and piretanide.

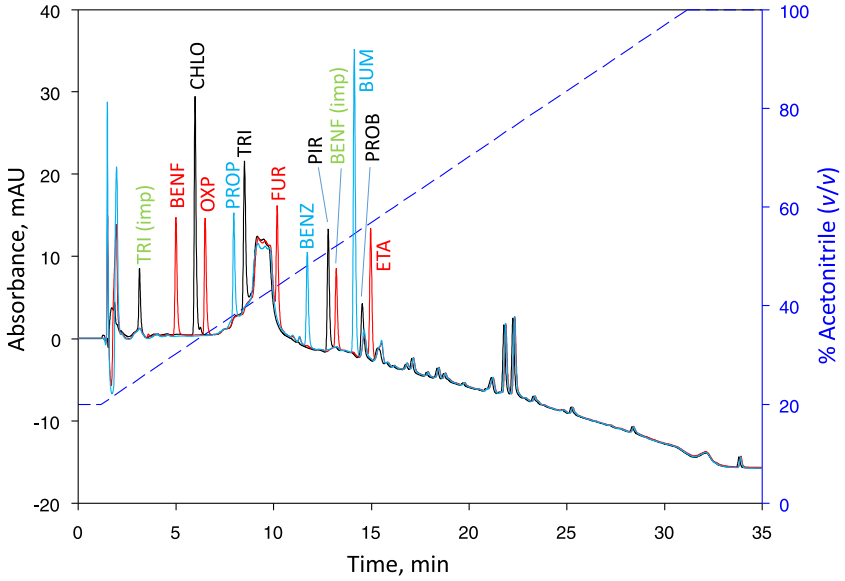

Fig. 2. Chromatograms corresponding to the mixture of diuretics and β-blockers, injected in three groups (depicted in red, blue and black) using gradient G1. Common peaks to the three injections corresponding to the 26 injector impurities are also observed. The degradation products of thiazides are labelled in green.

Table 2
Regression statistics and parameters of the individual and global models for the set of nine diuretics, two β-blockers and two thiazide degradation products, based on the Neue-Kuss equation. Uncertainties obtained in the prediction of Mean deviations and relative mean deviations comparing predicted and experimental retention times with the six training gradients. The compounds are listed according to the elution order observed in the scouting gradient (see Fig. 1).

Compound	*R*	*F*-Snedecor	SEP	Mean deviation, min	Relative mean deviation, %	log k_0	*b*	*c*
	Individual models							
Trichloromethiazide (imp)	0.893320	18	0.01	0.006	0.19	1.699	1.717	5.077
Bendroflumethiazide	0.975317	62	0.05	0.034	0.66	1.215	1.270	1.911
Chlortalidone	0.998461	955	0.05	0.033	0.51	1.148	1.862	0.343
Oxprenolol	0.999829	8702	0.03	0.017	0.23	1.126	2.084	-0.232
Propranolol	0.999906	15982	0.04	0.022	0.24	2.027	5.668	4.546
Trichloromethiazide	0.999476	2828	0.07	0.048	0.49	1.725	3.441	3.442
Furosemide	0.999991	165172	0.02	0.011	0.09	1.556	3.628	1.736
Benzothiazide	0.999996	357526	0.02	0.008	0.05	1.522	3.846	1.468
Piretanide	0.999972	53864	0.05	0.030	0.18	1.987	6.692	3.750
Bendroflumethiazide (imp)	0.999995	304717	0.02	0.134	0.08	1.388	3.720	0.859
Bumetanide	0.999997	537641	0.02	0.010	0.05	1.689	5.258	1.922
Probenecid	0.999910	16798	0.10	0.058	0.31	2.450	11.68	7.752
Ethacrynic acid	0.999973	56466	0.06	0.038	0.20	1.794	5.801	2.550
	Global model							
Trichloromethiazide (imp)	< 0.9	9	0.02	0.016	0.50	1.339	0.1218	13.94
Bendroflumethiazide	< 0.9	8	**0.27**	0.166	3.26	1.737	0.1218	13.94
Chlorthalidone	0.995040	347	0.10	0.055	0.85	1.958	0.1218	13.94
Oxprenolol	0.999262	1903	0.06	0.032	0.44	2.064	0.1218	13.94
Propranolol	0.994642	233	**0.29**	0.186	1.96	2.343	0.1218	13.94
Trichloromethiazide	0.988710	172	**0.34**	0.216	2.23	2.351	0.1218	13.94
Furosemide	0.999925	20380	0.05	0.026	0.21	2.650	0.1218	13.94
Benzothiazide	0.999938	24470	0.06	0.037	0.25	2.881	0.1218	13.94
Piretanide	0.999578	3437	**0.20**	0.135	0.81	3.070	0.1218	13.94
Bendroflumethiazide (imp)	0.999979	71703	0.05	0.030	0.18	3.101	0.1218	13.94
Bumetanide	0.999927	20297	0.09	0.056	0.30	3.248	0.1218	13.94
Probenecid	0.999856	10651	0.13	0.070	0.37	3.297	0.1218	13.94
Ethacrynic acid	0.999840	9515	0.14	0.072	0.37	3.360	0.1218	13.94

In general, both the individual and global models provided fairly similar descriptions, despite the difference in the number of parameters, 39 for the 13 individual models (13 × 3), and 15 for the global model (13+2). Global models have the advantage that can be extended to include other constituents, present or not in the original sample, but with the drawback of not predicting changes in elution order (at least in the current state of the research). The next section examines how these benefits and drawbacks are translated in the optimisation of the separation performance.

4.3. Optimisation of the resolution using individual and global models

The optimisation of the peak purity for the probe mixture was carried out by applying Genetic Algorithms, using first the product of global peak purities as COF. In order to obtain the experimental conditions to get the best performance, a Pareto plot (Fig. 4) was drawn. This is a common tool used in optimisations including conflicting objectives (in this case, maximal global peak purity and minimal analysis time). In the figure, each gradient is represented

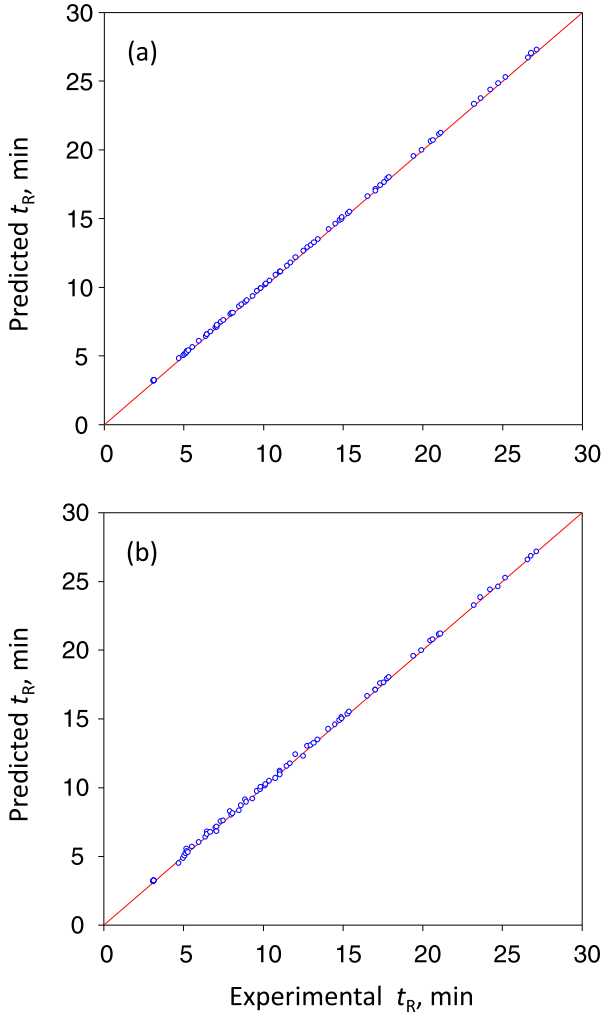

Fig. 3. Correlation between experimental and predicted retention times, using: (a) the individual models for each of the 13 probe compounds (11 analytes and two thiazide impurities), and (b) a single global model, resulting from the application of the alternate regression strategy to the 13 probe compounds. Fitting statistics (n = 78): (a): R = 0.99998, F = 2724595, standard error in prediction (SEP) = 0.035, and (b): R = 0.99983, F = 217175, SEP = 0.124.

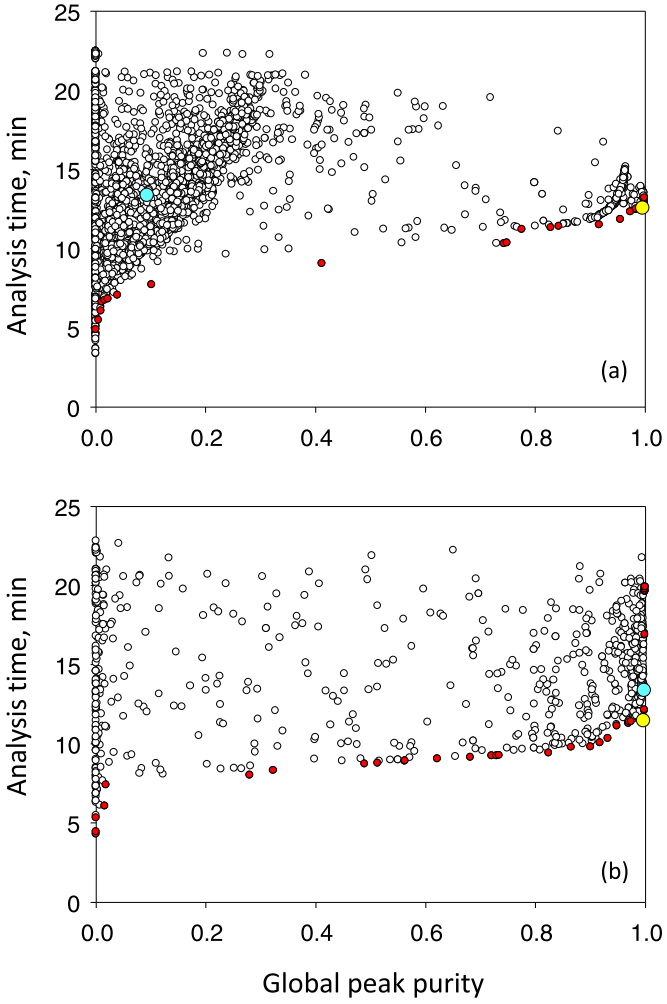

Fig. 4. Optimisation of the peak purity for the mixture of diuretics and β-blockers using: (a) the restricted global model, or (b) the 13 individual retention models, which offer a more accurate description, since the behaviour of each solute is modelled specifically. The Pareto fronts (in red), and optimal gradients that get maximal purity values in a minimal time (in yellow), are shown for both types of models. Both optimisations selected the same optimal gradient with three nodes in the first linear segment of the base gradient (see Fig. 5). A gradient marked in blue is also highlighted (see text for discussion). The number of generations needed to reach convergence was: (a) 31, and (b) 22, both using 100 gradients by generation.

by a dot. A series of gradients have been highlighted in red, defining a boundary called "Pareto front", which includes those gradients where the peak purity cannot be improved without worsening the analysis time, or vice versa.

Fig. 4 shows the separation performance of the population of all gradients that, in mutual competition, were evolved and examined throughout the optimisation along about 20 generations. The timescale was reduced from 30 to 20 min to expedite the analysis. The elution program (min, % acetonitrile) used to obtain the base chromatogram was: [(0, 20), (20, 100), (30, 100), (30.01, 20), (50, 20)] (the real times at the column inlet are obtained by adding the dwell time, t_d, which gives rise to an initial isocratic segment). During the optimisation, three nodes were inserted between the two first nodes in the base gradient (i.e., between 0 and 20 min, plus t_d), whose positions were varied to improve the separation performance. Therefore, the full gradient included four consecutive ramps that replaced the first segment of the base gradient (see for example Fig. 5, where the inserted nodes are marked in blue).

Among the gradients in the Pareto front, that one giving rise to almost complete resolution among peaks in the most reasonable time is marked in yellow. Note that for the given example, both the optimisation based on the global model (Fig. 4a) and on the 13 individual models (Fig. 4b) selected the same gradient balancing both analysis time and resolution. It should be noted that both optimisations were independent and examined different gradients along their evolution; nevertheless, they found the same optimal gradient (see the simulated chromatograms in Fig. 5). However, the usual case would be finding similar, but not exactly coincident gradients because the two populations and their evolutions are random and independent.

From the comparison of the Pareto plots for the restricted global model and the 13 individual retention models, it is observed that, in general, the gradients that offer maximal peak purity tend to coincide, although the global model offers fewer favourable gradients, and as a consequence, there is a larger accumulation of gradients with low peak purity. The differences arise from peak reversals, which currently global models cannot predict. Global model-based optimisations, thus, lead to fewer high-resolution gradients. This implies a loss of opportunities to find useful gradients that provide successful separations. Nevertheless, the more complex the sample, the less the importance of particular peak reversals in the overall solution, because the general separation is well predicted.

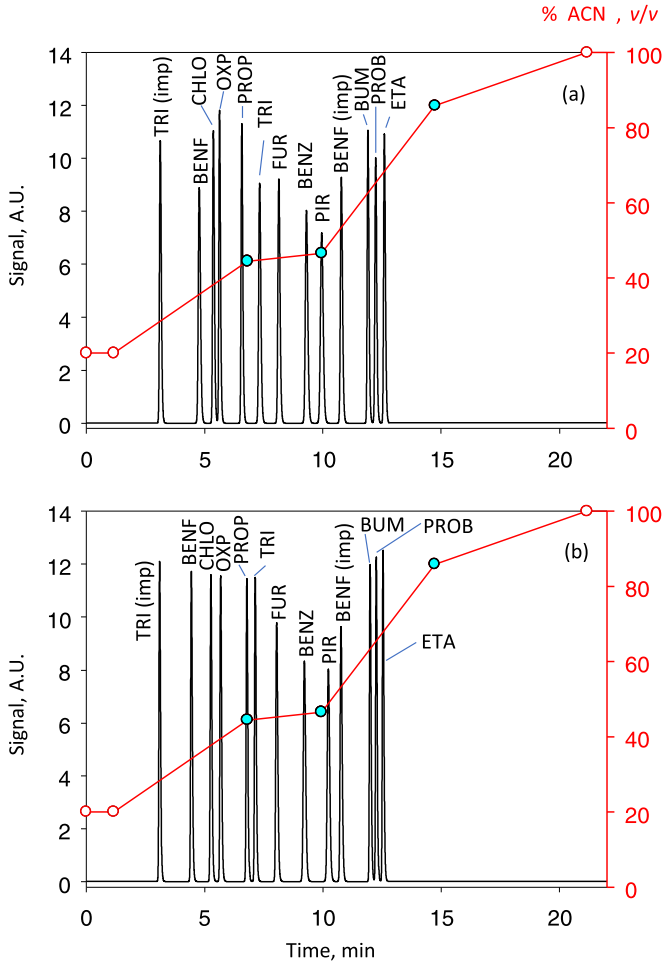

Fig. 5. Normalised optimal chromatograms obtained according to: (a) the restricted global model, and (b) the 13 individual retention models (one per solute). The best gradients found in independent optimisations, using the individual models on the one hand, and a single global model on the other, were identical, with $R = 0.995$ and an analysis time of 12.5 min.

If, for instance, a sample includes two hundred peaks, there will be unavoidably some of them overlapped or reversed. In such cases, the objective is not resolving all peaks, but obtaining a maximal separation even when some peaks are overlapped. This can be achieved with global models.

Fig. 6 shows an extreme example of differences in peak purity for chromatograms obtained with the same gradient (scores marked with blue dots in Fig. 4a and b), whose predictions with individual (Fig. 6a) and global (Fig. 6b) models are very different for the critical pair. The chromatograms involve the nine diuretics, two β-blockers and two thiazide impurities. As can be seen, the gradient is scored with a very different product of peak purities for the global model and the 13 individual models ($R = 0.1$ and 1.0, respectively). Fig. 6c shows the experimental chromatogram and contains, besides the standard peaks, a number of additional peaks coming from the injector contamination. The signals have been vertically shifted and scaled to allow a better comparison of peak positions. It can be seen that two of the constituents (trichlorometiazide and propranolol) are predicted with the global model as co-eluting, while the individual models predict them (correctly) separated. These two compounds stand out in Table 2 owing to their larger values of standard deviation in predictions (SEP), threefold larger as compared to the other compounds, when the experimental data were fitted to the global model. This fact denotes changes in selectivity along the experimental design that can give rise to changes in elution order. Note, however, that the overall separation is very similar.

Taking as correct the predictions offered by the individual models, it can be concluded that when the global model predicts complete separation, very likely the prediction will be correct because individual models also tend to predict high peak purity. On the contrary, a gradient with very low peak purity according to the global model denotes changes in selectivity, with possible changes in elution order when the gradient program is altered. In such cases, the individual models provide more reliable descriptions. In general, accurate predictions in situations of peak reversals are intrinsically more critical, leading to less reliable results: the actual separation could be better if the peaks completed the peak reversal process and separate gradually from each other in the reversed position. In general, the true separation performance tends to be better than the value predicted by the global model, since the scores in the region of low global resolution tend to concentrate in the upper part of the figure.

It should be commented that the optimisations in Fig. 4 were independent and involved different populations of gradients, giving rise to two independent historical (or cummulative) populations over the generations. The different populations made that both scores were not comparable to each other. To allow a comparison involving the same gradients, the same historical population was re-evaluated calculating peak purities with both types of retention models: the restricted global and the individual models (Fig. 7). The scores differ at low overall peak purity, but the predictions agree when it is high for the global model, so that the lower right quadrant is almost empty. This observation indicates the trend of the global models to offer reliable predictions if the value of overall peak purity is high, since when predicted with the individual models (the most accurate predictions) the resolution tends to be also high for the same gradients.

4.4. Global modelling of the peaks associated with the injector

The capability of global models to be extended to additional compounds gives rise to another interesting application: the possibility of modelling peaks whose identity may be unknown, and therefore, standards will rarely be available (e.g., unknown analyte impurities, matrix components, or metabolites in physiological fluids). As mentioned, the instrument used in this study presented a contamination problem: the presence of substances strongly retained in the injection system, which could not be eliminated even after careful and repeated washing with pure solvent at the maximal volume allowed by the injector. The presence of these reproducible peaks offered the opportunity to test the hypothesis of modelling the background or matrix peaks. Injections of acetonitrile were available with all the gradients included in Fig. 1, which were used to monitor the contamination level of the injector.

To create the extended global model (which describes the retention of the analytes and additional peaks), column and solvent parameters must first be obtained from a set of reference peaks. These parameters are specific for the separation system, organic modifier (type of solvent and concentration range), and column, these being $b = 0.1218$ and $c = 13.94$ for the Neue-Kuss model (Eq. (1)) in the studied example. These parameters were obtained by alternate regression [27], using the retention data of the 13 solutes as described previously. This type of regression makes the column and solvent parameters independent of the solutes, and therefore, these are potentially valid for additional solutes (even if no standards are available for them), provided that they are analysed with the same instrument, column and solvent. Next, the global model is extended to the rest of solutes (e.g., matrix, impurities), preferably using the information obtained with one of the slowest gradients in the design. In this way, a specific term in the

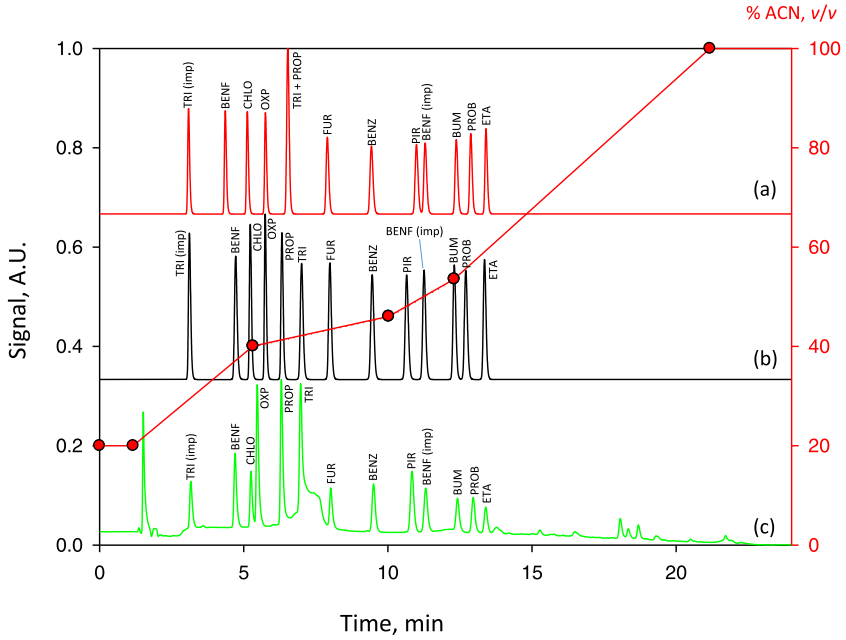

Fig. 6. Differences in the prediction of chromatograms associated to the same gradient, using: (a) the restricted global model for the 13 compounds (global resolution $R = 0.0937$, $t = 13.25$ min), and (b) 13 specific retention models, one per solute ($R = 0.9985$, $t = 13.40$ min). The experimental chromatogram, including the peaks associated with the injector contamination, was detected at 274 nm.

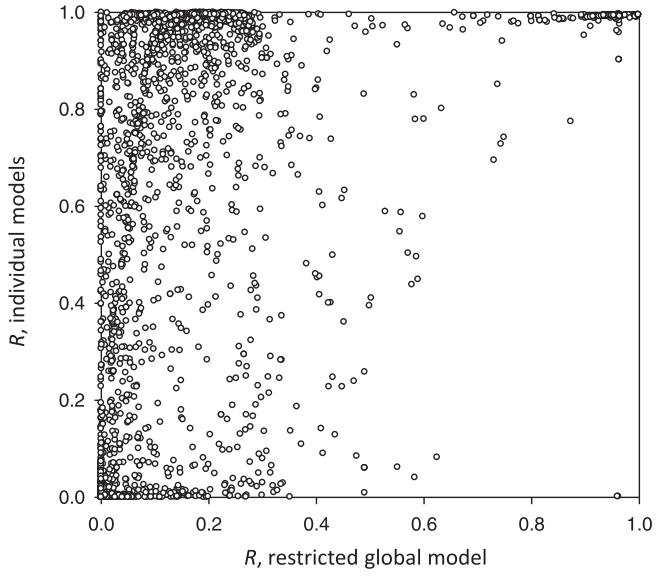

Fig. 7. Comparison between overall resolution scores (expressed as product of peak purities, R), when predictions are carried out with individual and global retention models. The 3100 gradients constituting the historical population of the optimisation carried out with Genetic Algorithms, using the restricted global model as predictor of the retention (Fig. 4a), were re-evaluated using the individual retention models as predictors.

Neue-Kuss model ($\log k_{0,i}$) is determined for each compound in the base chromatogram.

The ability of the extended global model to predict the changes in the distribution pattern of the contaminant peaks originated in the injector, produced by changes in the gradient program, was first evaluated. For this purpose, pure acetonitrile was injected using gradient G5 (a slow gradient). From this, the expected chromatogram for the injector contaminants obtained with another gradient profile (this time a fast gradient, G4) was predicted. Thus, the peaks of the impurities were predicted using the chromatogram of a slow gradient and the global parameters previously found for the restricted global model.

Some limitations should be remarked:

(i) Hydro-organic eluents in the gradient programs and pure acetonitrile present different solvation capabilities.

(ii) The use of global half-width plots forces all detected peaks (either true peaks, refractometric signals or associated with noise) to be processed as chromatographic signals associated with retained compounds. As a consequence, the predicted peaks tend to be higher and thinner with regard to those in the experimental chromatogram, which contain several wider bands, owing to the presence of accumulated unresolved compounds.

(iii) The data coming from the chromatogram auto-analysis MATLAB function were kept unmodified, so that anomalous peaks in the base chromatogram (e.g., merged peaks, refractometric signals), which were translated in anomalous predictions, are present. The default detection settings from the Matlab standard function “findpeaks” were applied to detect all peaks (e.g., distance from neighbouring peaks 0, critical height -∞, critical peak width 0, or critical prominence 0, –see the Matlab documentation–). Additional thresholds related to the detection conditions in Chromscan (a function developed in our laboratory) were added, such as discarding peaks below the 99.95% cumulative area, or with height below 5 times the noise once the baseline has been subtracted.

Fig. 8 shows the transference of the contamination background in the experimental chromatogram obtained with the slow gradient (Fig. 8a,b) to the chromatogram for a fast gradient (Fig. 8c,d). For this purpose, the experimental chromatogram for the slow gradient (Fig. 8a) was first acquired, and all visible peaks, auto-anaylised (detected and measured). Then, the extended global model including all the background peaks (but no analytes) was built, including 26 contamination peaks or peak clusters. This model, together with the global half-widths models, allows the prediction of the background expected for the slow gradient (Fig. 8d), which can be compared with the corresponding experimental chromatogram (Fig. 8c). The limitations previously com-

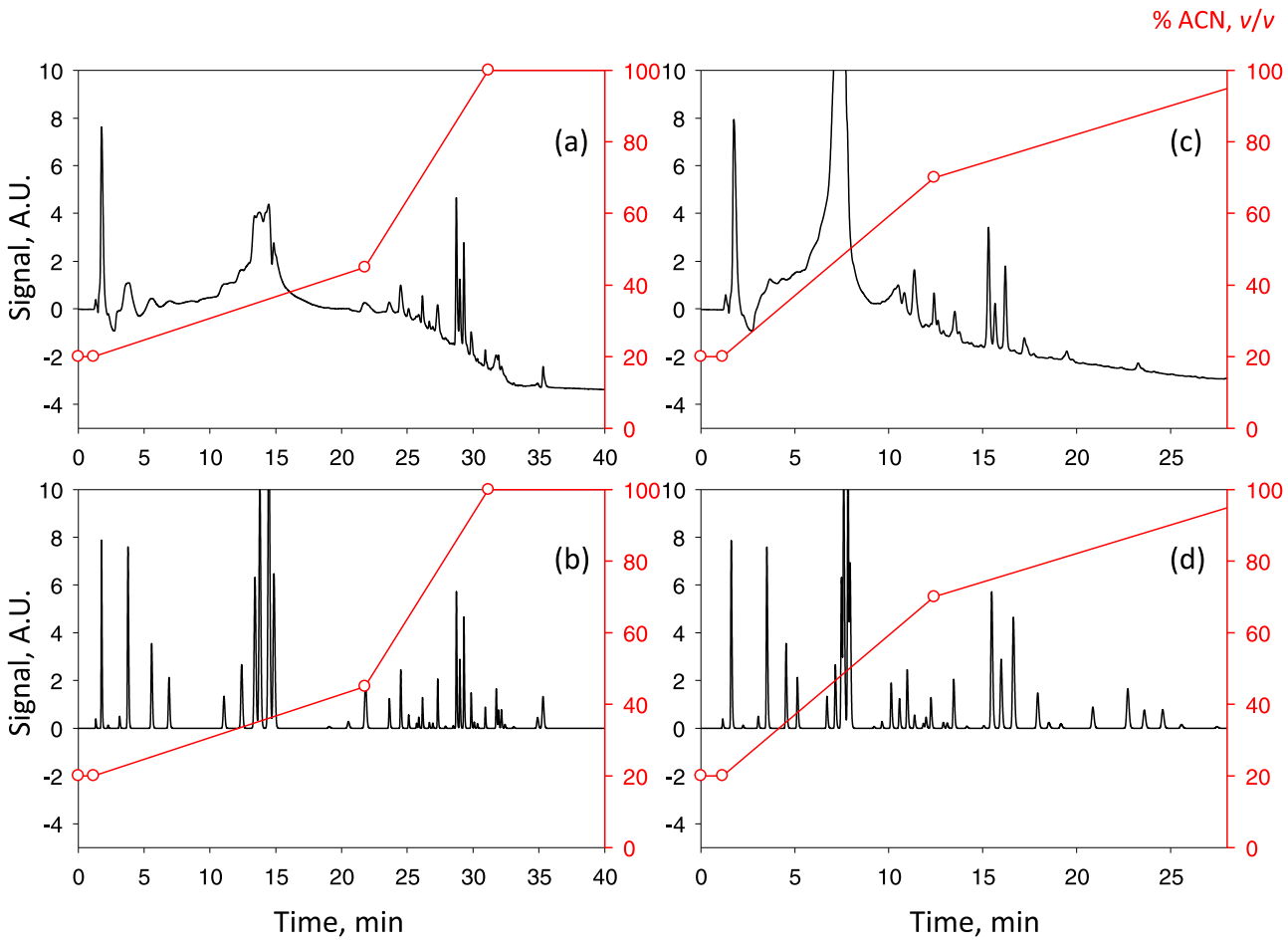

Fig. 8. Experimental (a,c) and predicted (b,d) chromatograms corresponding to the injector contaminants, obtained by injection of pure acetonitrile. Gradient G4 (c,d) is predicted using the global model extended from gradient G5 (a,b).

mented are visible: peaks for unresolved clusters are predicted as single narrow signals. The base chromatogram is modelled as shown in Fig 8b, where all auto-detected signals are predicted with the global half-width models, but there is no prediction of retention times.

In spite of all indicated limitations, the similarity between predicted and experimental chromatograms is satisfactory, before and after the transference. Therefore, developing an optimisation that takes into account the matrix or external peaks (as is the case of the injector contaminants) in the separation of the analytes is feasible, so that these are free from their mutual interference without co-elution with matrix or external peaks.

4.5. Optimisation of the separation of the analytes in the presence of the impurities associated with the injector

Three types of models were developed above: (i) the restricted global model associated with the 11 analytes and 2 degradation products (see the model parameters in Table 2), (ii) the extended global model for the contamination background (Fig. 8), and (iii) the 13 individual models associated to the analytes and degradation products. Based on these models, different optimisation strategies can be applied for the set of analytes. For instance:

(i) A direct optimisation based on the extended global model, which includes the peaks of the 13 analytes and 26 background peaks altogether, giving rise to a combined global model. This combined model should be preferably obtained from the chromatogram of the slowest gradient in the experimental design, by analysing the mixture of the analyte standards and the thiazide impurities. When such solution is injected, the injector contaminants are inserted in the sample, and thus, all peaks will be visible in the chromatogram (see for instance Fig. 3, where the standards were injected in three groups).

(ii) A hybrid optimisation, that combines the 13 individual models and the extended global model for the background (the 26 peaks coming from the injector).

Naturally, strategy (i) can also be carried out by combining the results of separate injections of the analytes (individual solutions or mixed incompatible groups), on the one hand, and the matrix (blank solution or pure solvent), on the other. Fig. 9 shows the results of strategy (ii) which, as in previous cases, was obtained after optimising three nodes that replaced the first linear segment of the base gradient. The peaks originated by the injector could be excluded from the sum of peak purities, so that their effects have no impact on the separation level of the analytes, regardless of the mutual overlapping level of the contaminants. In this way, the contaminants would not affect the sum of purities, as long as they do not overlap with one or more analytes. Either using the extended global model (strategy (i)), or hybridising a restricted global model developed only for the injector impurities, with the individual models that describe the retention of the analytes with high accuracy (strategy (ii)), a new way of optimising

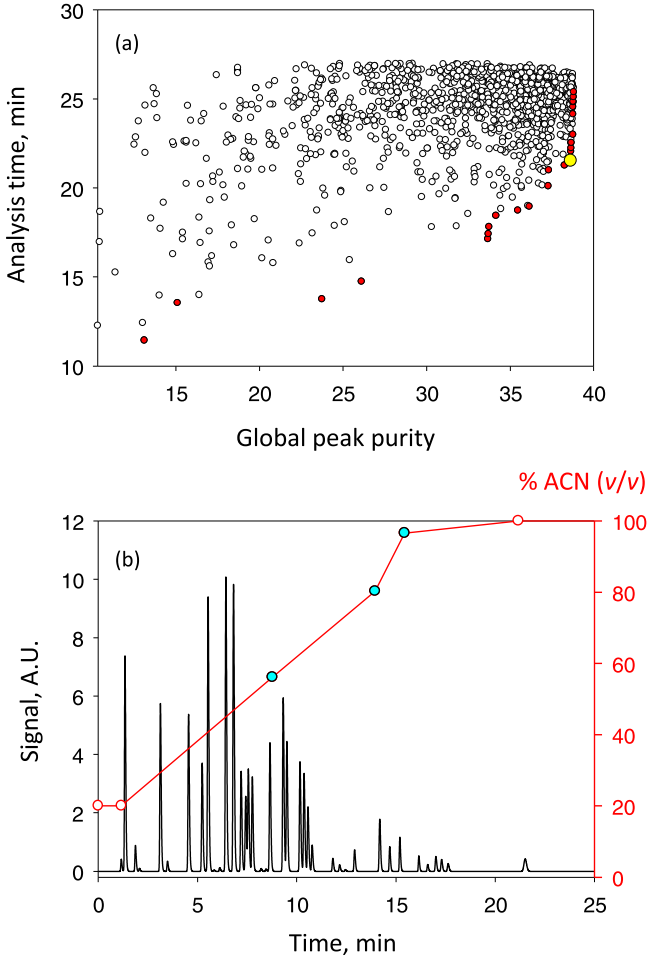

Fig. 9. Optimisation of the separation of a mixture of diuretics and β-blockers, including the effects of the matrix peaks (injector contaminants), based on the extended global model: (a) Pareto plot showing overall peak purities and analysis times for the historical population of gradients, and (b) chromatogram corresponding to the optimal gradient, whose performance is marked in yellow in (a). Three nodes had to be allocated in the first 20-min of the gradient program and optimised (0–20 min, 20–100% acetonitrile). The number of peaks included in the study was 39: the 11 analytes, the two degradation products, and the 26 most intense peaks associated with the injector contaminants.

the separation performance including the matrix is given, which is potentially useful for any type of sample.

5. Conclusions

The global retention model reported in Ref. [27] has a descriptive capability not too far from that of individual models, but with the possibility of being extended to new compounds, whenever the same chromatographic system (column, solvent and instrument) is used. The advantage of the individual models is that they are more adaptable to solute retention and can describe more accurately the effects of the media (column and eluent) on the retention of each solute, as a consequence of lacking common parameters. However, they have the drawback of requiring the repetition of the data acquisition process, when new solutes need being incorporated. On the other hand, it should be noted that conventional optimisations are not feasible for samples including a very high number of constituents. Also, global models only require one experimental condition to update the model, when one or several new compounds are added. The drawback of global models is that at least in their current state, they are not able to predict changes in elution order, but only peak co-elution.

The type of global model proposed in this work presents the advantage of being able to be extended to new solutes without the need of both knowing their identity and availing their chemical descriptors. It, however, has the inconvenience of not predicting changes in elution order. In contrast, hierarchical or multi-level models can predict changes in elution order but require knowledge of certain descriptors [30,31], which will be unknown for external or matrix peaks, or if the compound associated to the considered peak has not been characterised. In other words, there is no prediction without descriptors.

In this work, the problems associated with the optimisation of peak purity by applying global models, with no previous reports in the literature, are addressed. Optimisation results using global models are compared to a conventional optimisation, based on specific predictors for each compound. When the separation predicted by a global model was favourable, it was found that it tended to coincide with that predicted by the individual models, which describes the separation reliably. Moreover, if the separation performance predicted by the global model was poor, the actual separation was usually better. The larger the number of components in the sample, the more useful the global model, owing to its capability to offer good general predictions of retention.

Global models can constitute a way to incorporate matrix compounds in the optimisation. Some examples are: (i) the presence of endogenous compounds, or compounds resulting from the metabolism of drugs in physiological fluids, (ii) the inclusion of new members of a certain family of drugs in a screening study, or (iii) the modelling of a highly complex multi-analyte sample of a natural product. As mentioned, this type of model leads to the selection of conditions that offer good general separations, although it may fail for specific solutes, and implies accepting the loss of potentially valid separation conditions (gradients). However, it should be considered that the more complex the sample, the smaller the importance of particular miscalculations.

It has been experimentally verified that the prediction of separations expected using global models show good agreement, and the optimisation is reliable enough. The optimisation of the separation performance of fingerprint chromatograms using global models will be the subject of a new report (Part II).

Author contributions

Pau Peiró-Vila: Collected the data, Wrote the paper
María Daniela Villamonte: Collected the data
Isabel Luján-Roca: Collected the data, Wrote the paper
José Ramón Torres-Lapasió: Conceived and designed the analysis, Contributed data or analysis tools, Performed the analysis, Wrote the paper, Laboratory management
María Celia García-Álvarez-Coque: Conceived and designed the analysis, Wrote the paper, Laboratory management

Declaration of Competing Interest

The authors declare that they have no known competing financial interests or personal relationships that could have appeared to influence the work reported in this paper.

Data availability

The data that has been used is confidential.

Acknowledgements

Work supported by Grant PID2019-106708GB-I00 funded by MCIN (Ministery of Science and Innovation of Spain)/AEI/10.13039/501100011033. María Daniela Villamonte

thanks CONICET (dependent on the Ministery of Science, Technology and Innovation of Argentina) for a stay grant in the University of Valencia.

Supplementary materials

Supplementary material associated with this article can be found, in the online version, at doi:10.1016/j.chroma.2022.463756.

References

[1] P.J. Schoenmakers, Optimisation of Chromatographic Selectivity: A Guide to Method Development, Elsevier, Amsterdam, 1986.
[2] A.M. Siouffi, R. Phan-Tan-Luu, Optimization methods in chromatography and capillary electrophoresis, J. Chromatogr. A 892 (2000) 75–106.
[3] R. Cela, E.Y. Ordoñez, J.B. Quintana, R. Rodil, Chemometric-assisted method development in RPLC, J. Chromatogr. A 1287 (2013) 2–22.
[4] J.R. Torres-Lapasió, M.C. García-Alvarez-Coque, Liquid chromatography: strategies for optimization, in: P.J. Worsfold, A. Townshend, C. Poole, M. Miró (Eds.), Encyclopedia of Analytical Science, 3rd ed., Elsevier, Waltham, MA, 2019, pp. 252–260.
[5] S.N. Deming, S.L. Morgan, Experimental Design: A Chemometric Approach, 2nd ed., Elsevier Science, Amsterdam, 1993.
[6] D.B. Hibbert, Experimental design in chromatography: a tutorial review, J. Chromatogr. B 910 (2012) 2–13.
[7] J.A. Navarro-Huerta, A. Gisbert-Alonso, J.R. Torres-Lapasió, M.C. García-Alvarez–Coque, Testing experimental designs in liquid chromatography (I): development and validation of a method for the comprehensive inspection of experimental designs, J. Chromatogr. A 1624 (2020) 461180.
[8] A. Gisbert-Alonso, J.A. Navarro-Huerta, J.R. Torres-Lapasió, M.C. García-Alvarez–Coque, Testing experimental designs in liquid chromatography (II): influence of the design geometry on the prediction performance of retention models, J. Chromatogr. A 1654 (2021) 462458.
[9] M.C. García-Alvarez-Coque, J.R. Torre-Lapasió, J.J. Baeza-Baeza, Modelling of retention behaviour of solutes in micellar liquid chromatography, J. Chromatogr. A 780 (1997) 129–148.
[10] M.C. García-Alvarez-Coque, J.R. Torres-Lapasió, J.J. Baeza-Baeza, Models and objective functions for the optimisation of selectivity in reversed-phase liquid chromatography, Anal. Chim. Acta 579 (2006) 125–145.
[11] P. Nikitas, A. Pappa-Louisi, Retention models for isocratic and gradient elution in reversed-phase liquid chromatography, J. Chromatogr. A. 1216 (2009) 1737–1755.
[12] E. Tyteca, J. De Vos, N. Vankova, P. Cesla, G. Desmet, S. Eeltink, Applicability of linear and nonlinear retention-time models for reversed-phase liquid chromatography separations of small molecules, peptides, and intact proteins, J. Sep. Sci. 39 (2016) 1249–1257.
[13] M.J. den Uijl, P.J. Schoenmakers, B.W.J. Pirok, M.R. van Bommel, Recent applications of retention modelling in liquid chromatography, J. Sep. Sci. 44 (2021) 88–114.
[14] R. Cela, C.G. Barroso, J.A. Pérez-Bustamante, Objective functions in experimental and simulated chromatographic optimization: comparative study and alternative proposals, J. Chromatogr. 485 (1989) 477–500.
[15] S. Carda-Broch, J.R. Torres-Lapasió, M.C. García-Alvarez-Coque, Evaluation of several global resolution functions for liquid chromatography, Anal. Chim. Acta 396 (1999) 61–74.
[16] R.D. Caballero, S.J. López-Grío, J.R. Torres-Lapasió, M.C. García-Alvarez-Coque, Single-peak resolution criteria for optimization of mobile phase composition in liquid chromatography, J. Liq. Chromatogr. Rel. Technol. 24 (2001) 1895–1919.
[17] J.T.V. Matos, R.M.B.O. Duarte, A.C. Duarte, A generalization of a chromatographic response function for application in non-target one- and two-dimensional chromatography of complex samples, J. Chromatogr. A 1263 (2012) 141–150.
[18] E. Tyteca, G.A. Desmet, Universal comparison study of chromatographic response functions, J. Chromatogr. A 1361 (2014) 178–190.
[19] T. Alvarez-Segura, A. Gómez-Díaz, C. Ortiz-Bolsico, J.R. Torres-Lapasió, M.C. García-Alvarez-Coque, A chromatographic objective function to characterise chromatograms with unknown compounds or without standards available, J. Chromatogr. A 1409 (2015) 79–88.
[20] J.R. Torres-Lapasió, J.J. Baeza-Baeza, M.C. García-Alvarez-Coque, A model for the description, simulation and deconvolution of skewed chromatographic peaks, Anal. Chem. 69 (1997) 3822–3831.
[21] J.R. Torres-Lapasió, J.J. Baeza-Baeza, M.C. García-Alvarez-Coque, Modeling of peak shape and asymmetry, in: L. Komsta, Y. Vander Heyden, J. Sherma (Eds.), Chemometrics in Chromatography, CRC Press, Taylor and Francis Group, Boca Raton, FL, 2018, pp. 217–238.
[22] L.R. Snyder, J.J. Kirkland, J.L. Glajch, Practical HPLC Method Development, 2nd ed., John Wiley & Sons, New York, 1997.
[23] P.J. Schoenmakers, H.A.H. Billiet, R. Tussen, L. de Galan, Gradient selection in reversed-phase liquid chromatography, J. Chromatogr. A 149 (1978) 519–537.
[24] U.D. Neue, H.J. Kuss, Improved reversed-phase gradient retention modeling, J. Chromatogr. A 1217 (2010) 3794–3803.
[25] E. Bosch, P. Bou, M. Rosés, Linear description of solute retention in reversed-phase liquid chromatography by a new mobile phase polarity parameter, Anal. Chim. Acta 299 (1994) 219–229.
[26] P. Jandera, T. Hájek, M. Ružičková, Retention models on core-shell columns, J. AOAC Int. 100 (2017) 1636–1646.
[27] A. Gisbert-Alonso, J.A. Navarro-Huerta, J.R. Torres-Lapasió, M.C. García-Alvarez–Coque, Global retention models and their application to the prediction of chromatographic fingerprints, J. Chromatogr. A 1637 (2021) 461845.
[28] A. Gisbert-Alonso, S. López-Ureña, J.R. Torres-Lapasió, M.C. García-Alvarez–Coque, Chromatographic fingerprint-based analysis of extracts of green tea, lemon balm and linden: I. development of global models without the use of standards, J. Chromatogr. A 1672 (2022) 463060.
[29] A. Gisbert-Alonso, A. Navarro-Martínez, J.A. Navarro-Huerta, J.R. Torres-Lapasió, M.C. García-Alvarez-Coque, Chromatographic fingerprint-based analysis of extracts of green tea, lemon balm and linden: II. Simulation of chromatograms using global models, J. Chromatogr. A 1684 (2022) 463561.
[30] Ł. Kubik, R. Kaliszan, P. Wiczling, Analysis of isocratic-chromatographic-retention data using Bayesian multilevel modeling, Anal. Chem. 90 (2018) 13670–13679.
[31] A. Kamedulska, Ł. Kubik, J. Jacyna, W. Struck-Lewicka, M.J. Markuszewski, P. Wiczling, Toward the general mechanistic model of liquid chromatographic retention, Anal. Chem. 94 (2022) 11070–11080.
[32] D. Brynn Hibbert, Genetic algorithms in Chemistry, Chemometr. Intell. Lab. Syst. 19 (1993) 277–293.
[33] P. Nikitas, A Pappa-Louisi, A Papageorgiou, A Zitrou, On the use of genetic algorithms for response surface modeling in high-performance liquid chromatography and their combination with the Microsoft Solver, J. Chromatogr. A 942 (2002) 93–105.
[34] T. Alvarez-Segura, S. López-Ureña, J.R. Torres-Lapasió, M.C. García-Alvarez–Coque, Multi-scale optimisation vs. genetic algorithms in the gradient separation of diuretics by reversed-phase liquid chromatography, J. Chromatogr. A 1609 (2020) 460427.
[35] T. Alvarez-Segura, E. Cabo-Calvet, J.R. Torres-Lapasió, M.C. García-Alvarez–Coque, An approach to evaluate the information in chromatographic fingerprints: application to the optimisation of the extraction and conservation conditions of medicinal herbs, J. Chromatogr. A 1422 (2015) 178–185.
[36] J.A. Navarro-Huerta, J.R. Torres-Lapasió, S. López-Ureña, M.C. García-Alvarez–Coque, Assisted baseline subtraction in complex chromatograms using the BEADS algorithm, J. Chromatogr. A 1507 (2017) 1–10.
[37] J.J. Baeza-Baeza, S. Pous-Torres, J.R. Torres-Lapasió, M.C. García-Alvarez-Coque, Approaches to characterise chromatographic column performance based on global parameters accounting for peak broadening and skewness, J. Chromatogr. A 1217 (2010) 2147–2157.
[38] J.J. Baeza-Baeza, M.J. Ruiz-Angel, M.C. García-Alvarez-Coque, S. Carda-Broch, Half-width plots, a simple tool to predict peak shape, reveal column kinetics and characterise chromatographic columns in liquid chromatography: state of the art and new results, J. Chromatogr. A 1314 (2013) 142–153.
[39] G. Vivó-Truyols, J.R. Torres-Lapasió, A. van Nederkaassel, Y. Vander Heyden, D.L. Massart, Automatic program for peak detection and deconvolution of multi overlapped chromatographic signals: Part II: peak model and deconvolution algorithms, J. Chromatogr. A 1096 (2005) 146–155.
[40] P. Jandera, Predictive calculation methods for optimization of gradient elution using binary and ternary solvent gradients, J. Chromatogr. A 485 (1989) 113–141.
[41] R.G. Sammes, J.B. Taylor, Comprehensive Medicinal Chemistry, Vol. 6, Pergamon Press, Oxford, 1990.
[42] Molinspiration Property Engine: https://www.molinspiration.com/cgi-bin/properties (Molinspiration Cheminformatics, Slovenia)